6 March 2023

Dropsonde Data Report

Convective Processes Experiment - Cabo Verde
CPEX-CV (2022)

Holger Vömel

Earth Observing Laboratory
National Center for Atmospheric Research

Lee Thornhill, Claire Robinson

NASA Langley Research Center

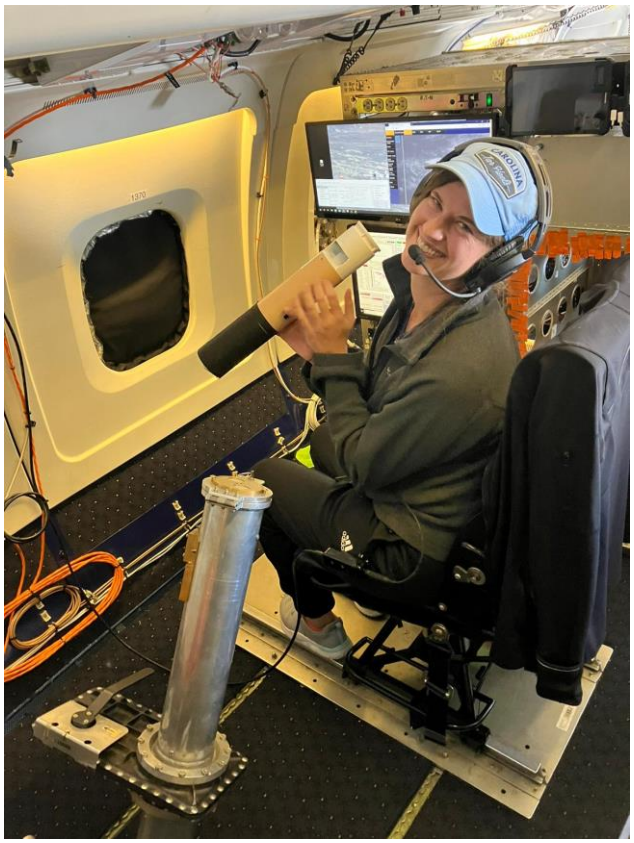

The dropsonde data for this project were quality controlled by the Earth Observing Laboratory at the National Center for Atmospheric Research (NCAR). The National Center for Atmospheric Research is managed by the University Corporation for Atmospheric Research and sponsored by the National Science Foundation.

Contact: Holger Vömel (voemel@ucar.edu)

Dropsonde Operators: Claire Robinson (NASA Langley), Lee Thornhill (NASA Langley)

Real-time dropsonde quality control: Alexis Wilson (U. Miami), Ariel Jacobs (U. Washington), Benjamin Rodenkirch (U. Wisconsin), Chu-Chun Huang (UC Davis), John Park (US. Navy), Margaret Hollis (U. Oklahoma), Nicholas Johnson (SUNY Albany), Quinton Lawton (U. Miami), Rebecca Beal (U. Utah), Rosimar Rios Berrios (NCAR), Sadiksha Rai (U. Oklahoma), Shu-Hua Chen (UC Davis), Shun-Nan Wu (U. Oklahoma), Tatiana Esteva-lngram (U. Oklahoma)

CPEX-CV at NASA ESPO:
https://espo.nasa.gov/cpex-cv/content/CPEX-CV

CPEX-CV at NASA GHRC:
https://ghrc.nsstc.nasa.gov/home/field-campaigns/cpex-cv

AVAPS dropsondes home page:
https://www.eol.ucar.edu/observing_facilities/avaps-dropsonde-system

Reference:

To refer to this data set or report, please use the following DOI:
https://doi.org/10.5067/ASDC/SUBORBITAL/CPEXCV-Dropsondes_1

Cover photo: Dropsonde launch onboard the NASA DC-8

Document Version Control

Version	Date	Author	Change Description
1.0	6 March 2023	H. Vömel	Initial Release

Table of Contents

1 Dataset overview

The Convective Processes Experiment - Cabo Verde (CPEX-CV) field campaign investigated atmospheric dynamics, marine boundary layer properties, convection, the dust-laden Saharan Air Layer, and their interactions across various spatial scales to improve understanding and predictability of process-level lifecycles in the data-sparse tropical East Atlantic region. The campaign used the NASA DC-8 research aircraft based at Sal Island, Cabo Verde, which carried remote sensing and in situ instruments to measure profiles of temperature, humidity, winds, aerosols and precipitation. One of the important datasets for this field campaign is the thermodynamic structure of the atmosphere measured by dropsondes released from the DC-8.

CPEX-CV used the RD41 dropsonde, which is the larger version of the dropsondes developed at NCAR. Between 6 September and 2 October 2022, 414 dropsondes were released from thirteen research flights, two transit flights and one test flight. Soundings were released from an altitude mostly around 12 km; however, some were launched at lower altitudes with the lowest release at 4.5 km. A total of 343 soundings provided complete vertical profiles of all parameters with a nominal vertical resolution between 5 to 6 m from the surface to almost flight altitude.

All flight tracks excluding the test flight out of the Armstrong Flight Research Center, CA, are shown in Figure 1.

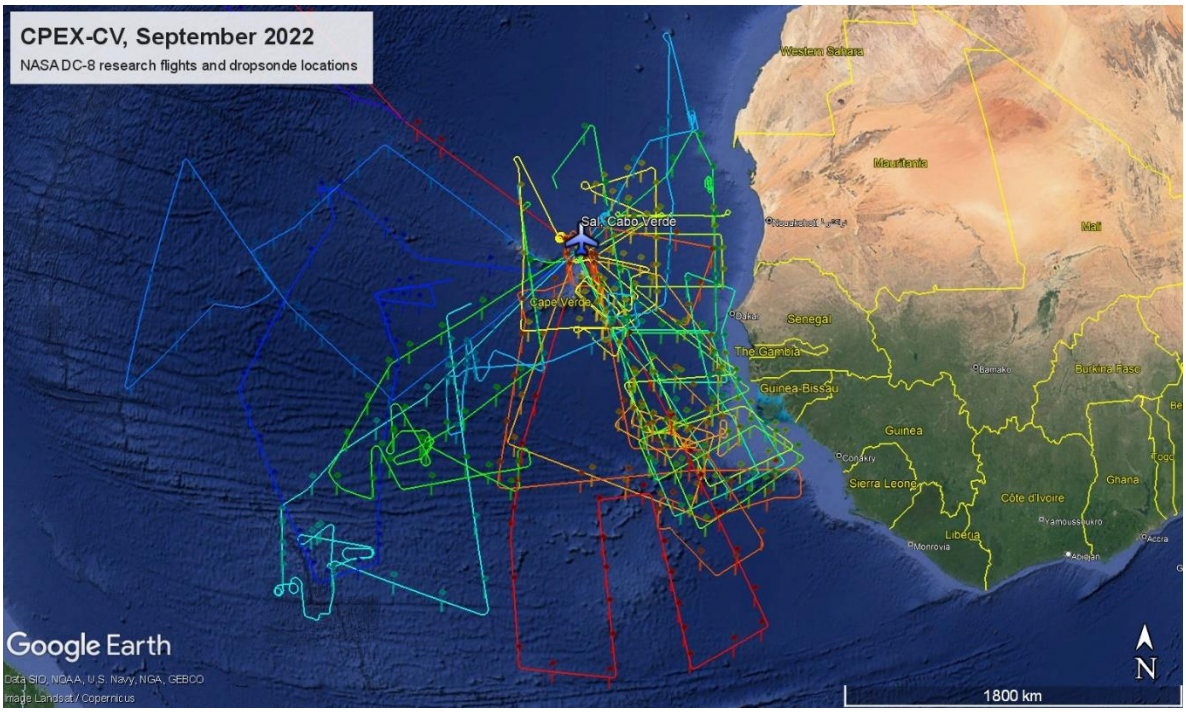

Figure 1: Flight tracks and locations of dropsonde releases during CPEX-CV

Table 1 provides an overview over all RD41 dropsondes released during CPEX-CV. Up to 43 sondes were launched on research flights. All soundings are listed in Appendix A.

Table 2 provides an overview of the performance of the dropsonde system as a whole. In total, 414 RD41 dropsondes were released from the aircraft. Of these, 48 soundings suffered damage or did not detect launch. In five soundings, the telemetry signal could not be tracked to the surface and in four the humidity sensor failed throughout the entire profile. In 10 soundings the GPS receiver failed for most or all of the profile to provide winds. 345 sondes reported complete atmospheric profiles to the surface.

The overall success rate of the dropsonde system for this campaign is at 83%.

Table 1: Overview over all flights releasing dropsondes during CPEX-CV

Research Flight	Date	# of Sondes	# of good sondes
TF01	16 Jun	3	3
TRANSFER	03 Sep	5	5
RF01	06 Sep	34	33
RF02	07 Sep	28	27
RF03	09 Sep	32	25
RF04	10 Sep	24	21
RF05	14 Sep	30	25
RF06	15 Sep	15	13
RF07	16 Sep	29	26
RF08	20 Sep	26	23
RF09	22 Sep	29	28
RF10	23 Sep	43	38
RF11	26 Sep	38	31
RF12	29 Sep	36	31
RF13	30 Sep	37	32
TRANSFER	02 Oct	5	5
Total		414	366

Table 2: Overview of the dropsonde system performance

	# of Sondes	Percent
Total number of sondes released	414	100
Successful releases	366	88
Complete thermodynamic profiles to the ground	355	86
Complete wind profiles to the ground	345	83

2 Dropsonde sounding system

For CPEX-CV, an NCAR 8-channel AVAPS® dropsonde system was installed aboard the NASA DC-8 research aircraft using a manual dropsonde launch tube for the Vaisala produced RD41 dropsonde model, which has been developed by NCAR in parallel with the smaller NRD41.

This dropsonde uses the pressure, temperature, and humidity sensor of the Vaisala RS41 radiosonde and employs an improved version of the GPS and telemetry. The parachute release of the RD41 relies on a ribbon delay system, which has been in use since the 1980s. This dropsonde model is used operationally by NOAA and the Air Force hurricane hunters and by all international research groups deploying the NCAR developed dropsonde system.

The AVAPS LabVIEW based software system receives and stores data from the dropsondes, the aircraft data system, and the AVAPS receiving system, including a reference GPS.

All dropsonde humidity sensors should be reconditioned prior to launch. This process is unique to the xRD41 dropsondes and reduces the potential of humidity contamination to a minimum. If done properly, it assures the best measurement performance throughout the entire altitude and temperature range of the profiles.

The manual dropsonde launcher was installed in the rear of the NASA DC-8 and the AVAPS station just in front of the launcher, allowing the dropsonde operator to launch sondes while still seated. This launcher had been developed in the early 1990s and uses a 3.75” diameter tube. For CPEX-CV, the launch tube was modified, and GPS signals were re-radiated directly into the launch tube to support wind measurements after launch.

Profile data were transmitted to the ground after the completion of each drop. Dedicated quality control staff checked each sounding in near real time. Those of sufficient quality were sent to the Global Telecommunications System (GTS) of the WMO via a data portal, which had been set up by NCAR specifically for this project.

3 Quality control procedures

3.1 Standard quality control

Standard quality control in near real time and as part of the final data QC is based on the algorithms implemented in the ASPEN software. The following quality checks, corrections, and calculations are performed:

- Removal of outliers and suspect data points in pressure, temperature, humidity, zonal and meridional wind, latitude, and longitude
- Removal of data between release from the aircraft and equilibration with atmospheric conditions
- Dynamic correction to account for the lag of the RD41 temperature sensor using the appropriate coefficients for the RD41 dropsondes
- Dynamic correction to account for the sonde inertia in the determination of the wind profile using the appropriate parameters for the RD41 dropsondes
- Smoothing of pressure, temperature, humidity, zonal and meridional wind
- Recomputing of wind speed and wind direction after smoothing of the wind components
- Extrapolation of the last reported pressure reading to a surface pressure value (where possible), based on the fall rate of the sonde
- Recalculation of the geopotential height from the surface to the top of the profile
- Computing a vertical wind speed component

This campaign used the RD41 dropsonde, which has a faster temperature sensor and faster RH sensor than the older RD94 sondes. This has been considered in the final dropsonde QC by changing the ASPEN QC parameters for these two sensors. The equilibration time for the temperature and RH sensor has been adjusted to 10 s, and the smoothing wavelength for both parameters has been adjusted to 3 s.

3.2 Custom quality control

3.2.1 Missed launch-detect

The RD41 dropsondes launched in CPEX-CV suffered more failed launch-detects than expected based on previous campaigns. In 39 soundings (see Appendix A), the sonde did not detect its launch and as a result did not switch to high-power radio transmission resulting in loss of data reception within a short time are launch. The amount of data received by these soundings was low and the entire sounding was excluded from the data set as a result.

An investigation of all available engineering data indicates that the dropsondes suffered mechanical damage at launch, damaging the parachute detector. A review of the launch tube installed on the NASA DC-8 showed that the launch tube cap used during CPEX-CV is different than that used during OLYMPEX in 2015, when no such launch problems occurred.

Figure 2 shows the caps used in both campaigns. The cap installed during CPEX-CV used a mesh with 40% open space to cover the vent hole, whereas the cap used in OLYMPEX did not use a mesh. It may be hypothesized that the mesh restricted the air flow into the tube during the launch process, thereby slowing the speed at which the sondes are ejected. In addition, the speed at which sonde is ejected may depend on how fast the operator opens the gate valve of the launcher.

Almost all sondes were launched with the sensor module pointing downward, i.e. the parachute end cleared the aircraft last. At a lower ejection velocity, there is a possibility that the parachute end may have been damaged upon clearing the launch tube, thereby damaging the sensor.

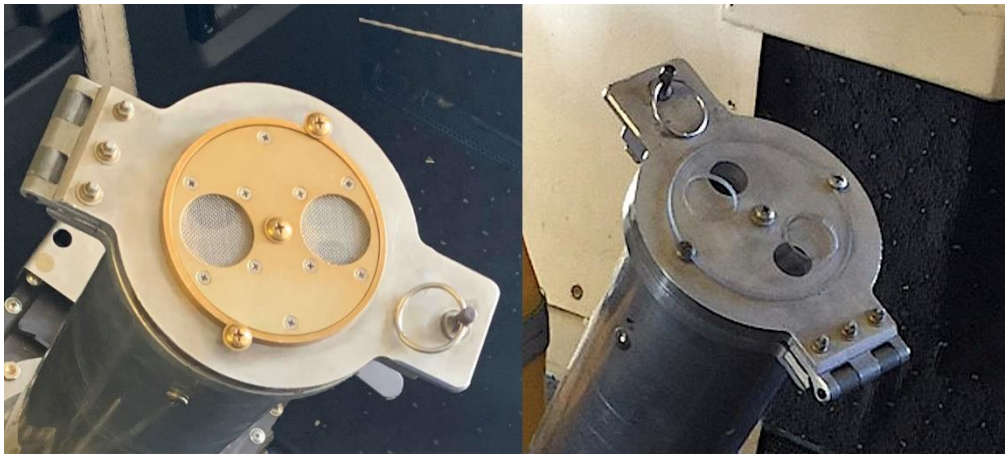

Figure 2: Cap on top of the dropsonde launch tube. Left: 2022 CPEX-CV; Right: 2015: OLYMPEX.

The use of the mesh and the level of opening the vent holes should be reviewed prior to the next campaign using this launch tube onboard a jet research aircraft.

3.2.2 Late launch-detect

Sounding 20220920_065544 experienced a late launch-detect related to the same issue discussed in the previous section. The launch time was changed from 06:55:44 to the correct time of 06:47:22. The time stamp has been changed in the metadata; the filename was not changed and reflects the incorrect launch time. The aircraft observations at the correct launch time were updated in the final data file. This sounding misses 6 minutes of data in the middle of the profile but contains a continuous profile after launch and before landing.

Users should note that file names should generally not be parsed to obtain launch date and time and should always refer to the metadata contained in the file for correct information.

3.2.3 PTU sensor failures

In three soundings, the temperature and humidity sensors failed at launch (Table 3). These soundings did not generate temperature and humidity observations and were excluded from the final data set. In four additional soundings, only the humidity sensor failed. In these soundings a temperature profile was transmitted. These soundings have been maintained in the final data set.

Table 3: Soundings, in which the temperature and humidity sensors fail

#	File	Failed sensor
1	20220906_171732	humidity
2	20220907_171047	humidity above 514 hPa level
3	20220923_095834	temperature, humidity
4	20220926_055242	pressure, temperature, humidity
5	20220926_080106	temperature, humidity
6	20220926_102814	humidity
7	20220930_132446	humidity
8	20221002_102228	humidity

3.2.4 Failed dropsondes

In six soundings, the dropsonde stops data transmission at launch (Table 4). These soundings generated no data and were excluded from the final data set.

Table 4: Soundings, in sonde stops data transmission at launch

#	File
1	20220906_112953
2	20220909_132450
3	20220909_153120
4	20220909_170002
5	20220916_192240
6	20220922_102303

3.2.5 Data gaps

Most research flights encountered periods during which the entire band between 400 and 406 MHz experienced strong interference. During these periods, reliable telemetry reception of dropsonde data was limited and data gaps occurred. The spectrum analyzer of the AVAPS dropsonde system shows a perfect correlation between the periods of interference and extreme humidity. Figure 3 shows as example the time sequence of the frequency spectrum overlaid with the relative humidity measurements onboard the aircraft. This sensor (EdgeTech model 137 Vigilant) measures total water, i.e. it evaporates ice particles entering the sensor generating very large apparent humidity increases when the aircraft flies in cirrus clouds. It is likely ice particles striking the aircraft generated p-static on the skin of the aircraft and interference on some or all communication systems, including the dropsonde telemetry system.

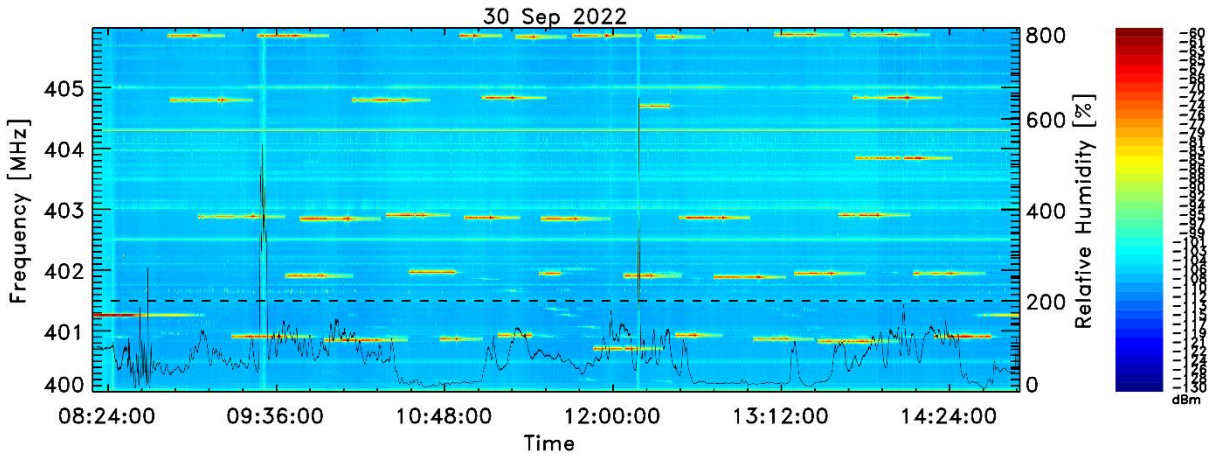

Figure 3: Spectrum analyzer time series (colors) and relative humidity (thin black line) reported by the aircraft data system. Horizontal red strips indicate the telemetry transmission of individual dropsondes. Two vertical light blue regions around 09:32:00 and around 12:11:00 indicate broadband interference signals affecting the entire band. Note the extreme spikes in relative humidity at the same time due to evaporating particles in the humidity sensor.

Data gaps ranged from as low as one second to many tens of seconds. In some cases, the data gaps occurred as dropsondes landed in the water. In these cases, measuring the exact surface pressure was not possible and the upward integration of the geopotential altitude was initialized using the last reported GPS altitude.

In several of these events, the telemetry reception of two dropsondes in the air at the same time was severely degraded. The telemetry reception of the dropsonde launched earlier was more strongly degraded than the later dropsonde, which was still closer to the aircraft.

3.2.6 GPS performance

The GPS receiver in the dropsondes operated properly in almost all sondes. During CPEX-CV, GPS signals were re-radiated directly into the launch tube of the DC-8. Therefore, there was no loss in GPS signal reception during the launch process and GPS speed measurements continued as a sonde was ejected from the aircraft.

In 10 sondes (Table 5), the GPS receiver was not able to measure a complete wind profile. In six of these, winds were removed entirely; in the other four, winds in only some layers were removed during quality control.

The accuracy of GPS wind measurements is slightly lower compared to the smaller NRD41, but still well within acceptable limits and better than 1 m/s. The filter in ASPEN was increased from its default of 0.6 m/s to 1.0 m/s for CPEX to minimize rejection of acceptable wind measurements.

Table 5: Soundings with missing wind observations

#	File	Comment
1	20220909_162708	No winds
2	20220915_184826	No winds
3	20220916_172129	No winds
4	20220920_055924	No winds above 7.1 km
5	20220920_061536	No winds above 7.2 km
6	20220922_073503	No winds between 2.1 and 8.7 km
7	20220923_104454	No winds
8	20220923_122255	No winds
9	20220923_131210	No winds
10	20220929_092456	No winds between 4 and 9 km

3.2.7 Pressure validation

The pressure sensor of the RD41 dropsonde is known to have a small bias. This sensor bias is measured during the production of the dropsondes and a correction is stored in the sonde to minimize the bias during observation.

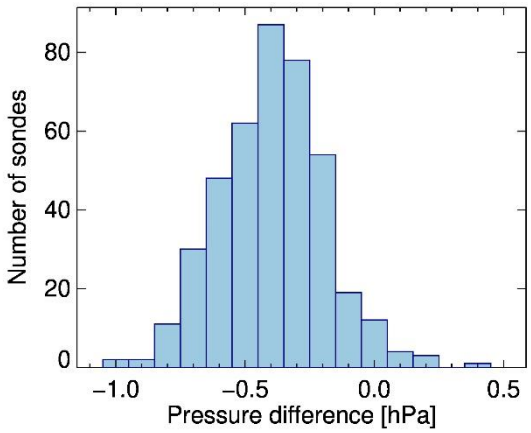

Figure 4: Pressure offset between the dropsonde and the reference sensor during production.

The statistics of the pressure bias measured and corrected during production is shown in Figure 4. The median pressure correction is - 0.39 hPa and the standard deviation 0.2 hPa. These measurements were used to correct the dropsonde pressure readings during production. Some drift between production and use of the sonde is possible, but still, the surface pressures reported by the dropsondes are expected to have only small systematic biases. The pressure inside the cabin or the launch tube was not measured and the pressure measurements of the dropsondes prior to launch could not be validated.

Five sondes (Table 6) did not use a production pressure correction. The real time pressure readings of these soundings may be low biased by up to 1.0 hPa. This correction was applied in post processing using the available metadata during production.

Table 6: Missing pressure offset correction applied in post processing

Research Flight	Sounding	Pressure offset applied [hPa]
RF01	20220906_131540	-0.40
RF04	20220910_202853	-0.57
RF05	20220914_105739	-0.26
RF05	20220914_135257	-0.21
RF09	20220922_063908	-0.58

During CPEX-CV, most sondes occasionally repeated a reported pressure measurement. This happened up to 19 times per sounding. While this is barely noticeable in any vertical profile, it did lead to additional noise in the calculated vertical fall rate. In post processing, these repeated pressure readings were interpolated, and the fall rates were recalculated. Only pressure readings had to be corrected. Temperature and relative humidity readings did not show any artificial repetition of measurements.

3.2.8 Relative humidity

The RH sensor on the xRD41 dropsondes should be reconditioned prior to launch. The sondes store the information, whether the reconditioning was successful, and we were able to verify that all sondes were properly reconditioned prior to take off before each flight. The humidity sensor in sounding 20220909_132450 was reconditioned 50 hours prior to launch, which is considered acceptable although not desirable. Any contamination in the sensor material was removed and the relative humidity sensors were expected to perform with negligible calibration drift.

The time response of the NRD41 relative humidity sensor is less than one second near the surface and up to 20 s at flight level of the NASA DC-8. A correction for this response time lag has not yet been implemented in ASPEN but was applied in post processing. The effect of this correction is noticeable at altitudes above approximately 10 km and strongly increases the reported relative humidity near the top of the profiles.

Figure 5 shows the average relative humidity profiles for all CPEX-CV soundings before the time lag correction (red) and after time lag correction (blue). The effect of the time lag correction becomes significant only above about 10 km, where the time constant of the sensor becomes large, and where the reported profile shows a consistent vertical gradient. At 11 km, the time lag correction increases the relative humidity from an average value of 43% to 52%, i.e. by a factor of 1.21. Ice saturation at that altitude is at about 66% relative humidity (over liquid), significantly more corrected profiles are ice supersaturated at that level, i.e. indicating the possibility of clouds.

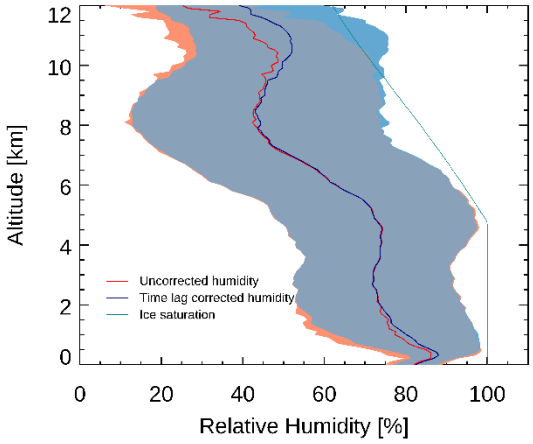

Figure 5: Mean relative humidity profile for all CPEX-CV soundings. The average of the uncorrected relative humidity is shown in red, the average of the time lag corrected relative humidity is shown in blue. The standard deviation for each is shown as shaded area.

We removed the first 10 s of the relative humidity and temperature profiles, while the sensors are equilibrating to the ambient environment. Lacking any validating observations, some uncertainty in the relative humidity at the top of the profile remains and we would estimate that the layer 300 m below the aircraft should be treated with caution.

3.2.9 Data from the surface

The RD41 dropsonde does not immediately sink to the ocean bottom and may transmit for a short time after landing in the water. These data must be manually filtered out, since they do not represent atmospheric observations. Fifteen soundings (Table 7) were identified, which contained data from the ocean surface that interfered with the filter algorithms built into ASPEN.

Table 7: Soundings containing data from the ocean surface. The last pressure reading is assumed to be above the surface.

#	File	Last Pressure [hPa]
1	20220906_170142	1008.69
2	20220909_135853	1011.99
3	20220909_162948	1008.67
4	20220909_163438	1009.18
5	20220909_165847	1010.25
6	20220909_184951	1007.94
7	20220910_151213	1010.05
8	20220910_172900	1009.91
9	20220914_130420	1008.30
10	20220920_074748	1008.41
11	20220923_111043	1009.85
12	20220923_115927	1006.05
13	20220926_083007	1007.64
14	20220926_092210	1009.72
15	20220929_082225	1009.85

4 Data file format

The files are provided in ICARTT format (https://www.earthdata.nasa.gov/esdis/esco/standards-and-practices/icartt-file-format) and are additionally archived at NCAR in NetCDF data files. These files are based on the Climate and Forecasting (CF) convention version 1.6 and compatible with any tool accepting this convention. The NetCDF data file format is described in Vömel et al. (2019).

5 Sounding metrics

5.1 Surface pressure

The surface pressure reported by the sondes is an extrapolation of the last measured air pressure above the surface to sea level using the current fall rate and is shown in Figure 6 as sequence of soundings and not as function of time. Soundings which did not provide data to the surface have been ignored here.

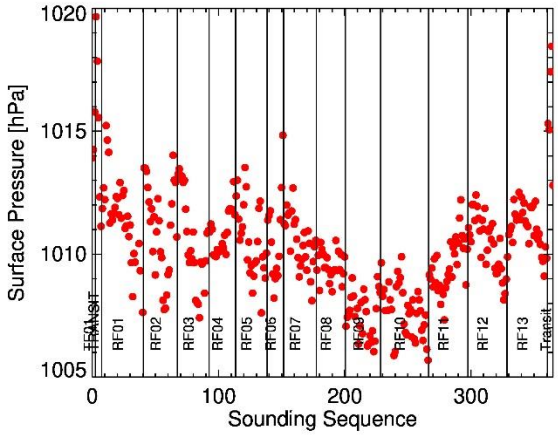

Figure 6: Surface pressure reported by all sondes reaching the surface.

5.2 Fall rate

A histogram of the fall speed near the surface is shown in Figure 7. The parachutes in all but five soundings functioned as expected. In two soundings, the parachutes failed completely and in three soundings the parachute opened significantly late (Table 8). The fall times had a median of 14.2 min and varied from 7 min for the fast-fall sounding to 15 min for the highest altitude sounding.

The fall rate decreases through the fall and sondes touch down in the water with a median of 10.0 m/s with a typical range of 9 to 11.5 m/s (Figure 7). The outliers above that range are the fast-fall sondes.

Table 8: Soundings with parachute failures

#	File	Partial fast-fall
1	20220906_164141	above 9 km
2	20220907_133732	
3	20220916_180341	above 4 km
4	20220922_080030	above 9.3 km
5	20220926_111944	

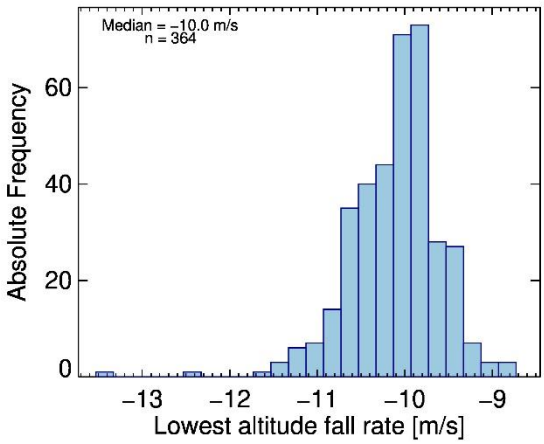

Figure 7: Distribution of the fall speed near the surface for all regular soundings.

5.3 Horizontal drift

Wind speeds during CPEX-CV were on average about 10 m/s and did not exceed 27 m/s in any sounding. No sounding reporting wind and position data traveled horizontally more than 17 km between release and landing (Figure 8).

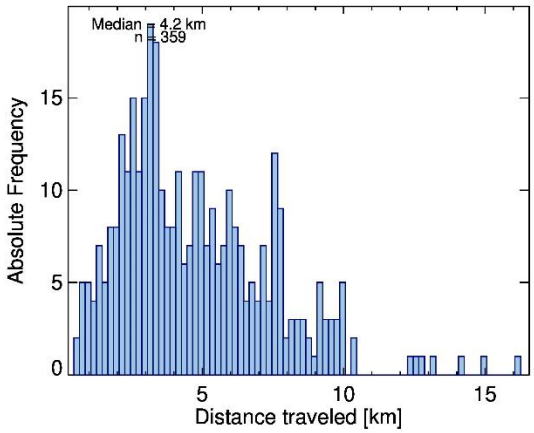

Figure 8: Distance between launch and landing for all dropsondes during CPEX-CV reporting winds.

6 Observations

6.1 Summary plots

Flights addressed different scientific goals. All observations provided profiles of pressure, temperature, relative humidity, horizontal winds and vertical winds. Figure 9 shows as example all 15 profiles from research flight 6 on 15 September. Vertical wind speeds were derived from the difference between the theoretical and the measured fall rate (Wang et al., 2008). The uncertainty of the technique is about 1 m/s and indicated as grey shaded area. In this example, only a layer of updraft at 19:52:49 UT at about 500 m is statistically significant.

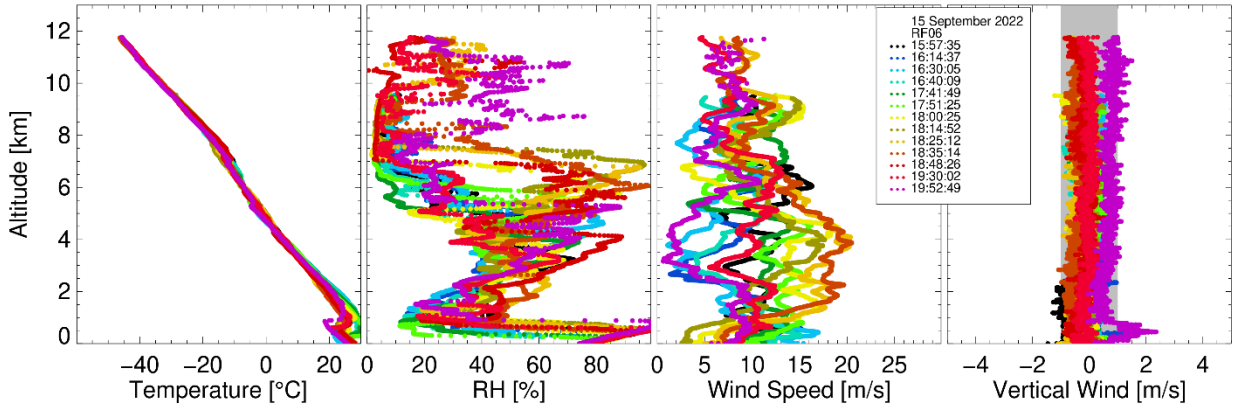

Figure 9: Dropsonde observations during RF06, 15 September 2022. Panels from left to right: Profiles of temperature, relative humidity, windspeed and vertical wind. Profiles of wind direction are not shown. The grey shaded area in the vertical wind plot indicates the estimated uncertainty of the derived vertical winds.

6.2 Temperature

The temperature measured by all dropsondes is shown as a contour plot in Figure 10. The individual research flights are separated by vertical lines. Temperatures at flight level were in the range of -10°C for the lower altitude drops to -54°C for the higher altitude drops. and near the surface in the range of +23°C to +30°C.

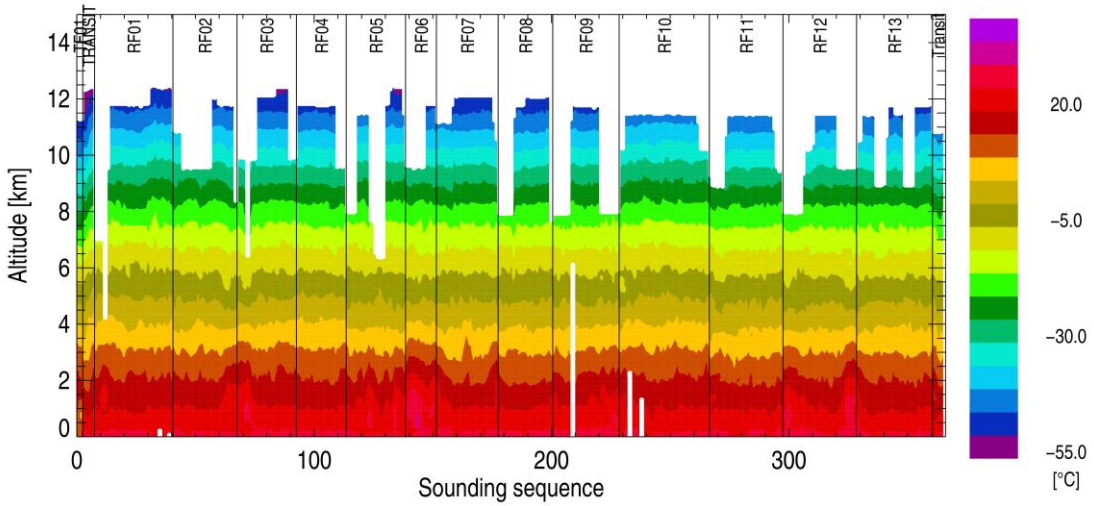

Figure 10: Color contours for all temperature measurements. All soundings are shown in the sequence in which they were released. The research flights are indicated near the top.

6.3 Relative humidity

Relative humidity reported by all dropsondes is shown in Figure 11. Below an air temperature 0°C relative humidity is expressed as relative humidity over ice instead of the conventional relative humidity over liquid water. Supersaturation with respect to ice indicates the likely presence of supercooled liquid or mixed phase clouds.

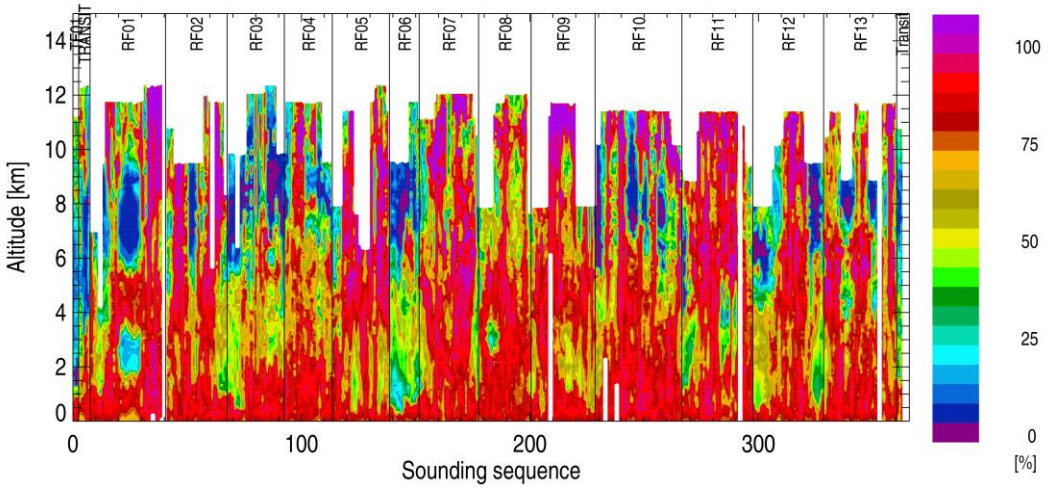

Figure 11: Color contours for relative humidity over ice

6.4 Winds

Zonal and meridional wind speeds are shown in Figure 12. The zero-wind line is indicated by a solid contour.

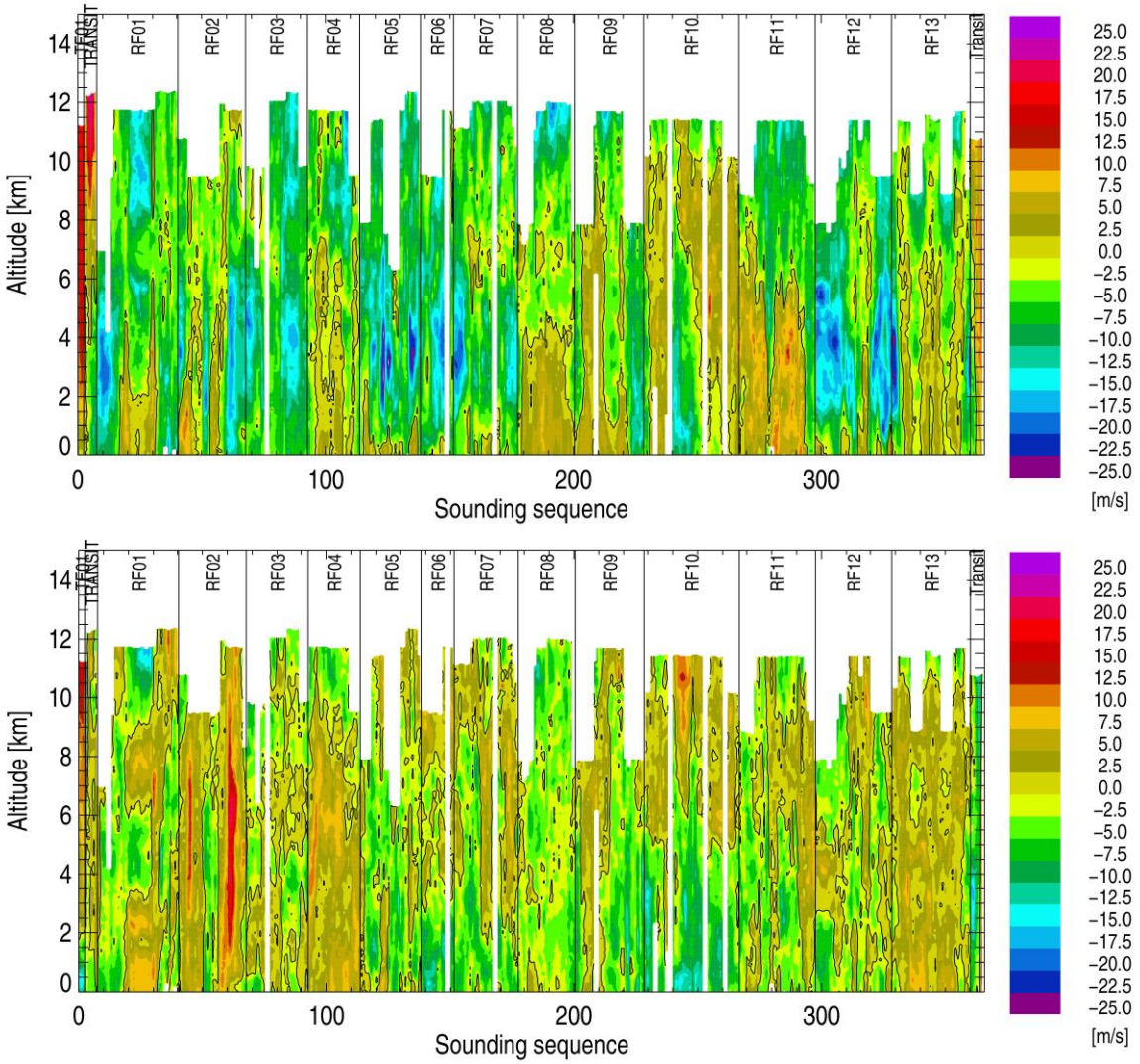

Figure 12: Color contours for all zonal (top) and meridional (bottom) wind speed measurements. Brown and red colors indicate westerly/southerly winds, green and blue colors indicate easterly/northerly winds.

6.5 Vertical winds

Dropsondes can sense stronger vertical winds. Several soundings showed significant updrafts and downdrafts throughout the profile (Figure 13, Figure 14).

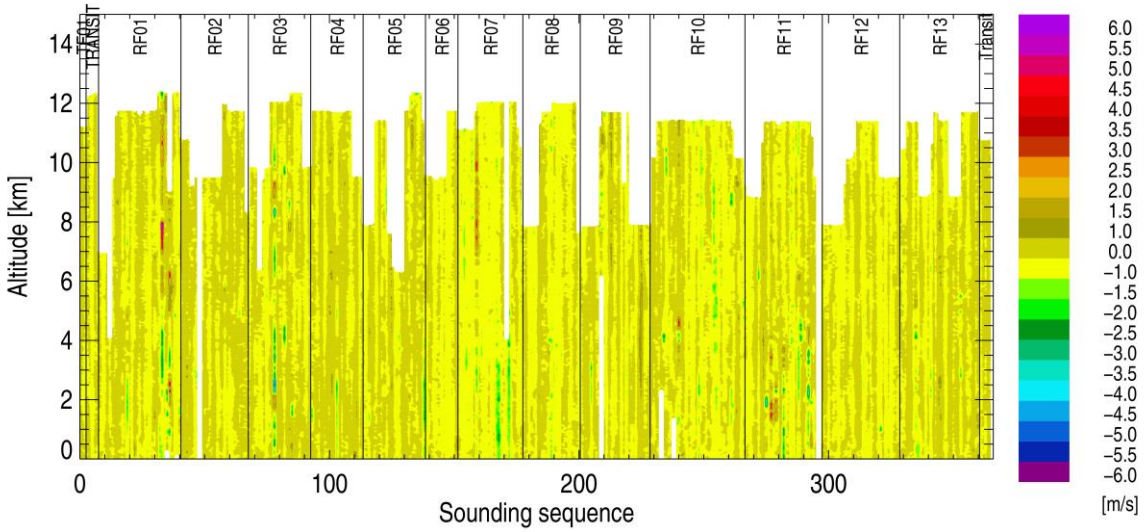

Figure 13: Vertical wind speed derived from the measured fall rate for all soundings with normal parachute performance. Colors other than yellow and brown indicate layers of upward (orange/red) or downward (green/blue) wind speeds.

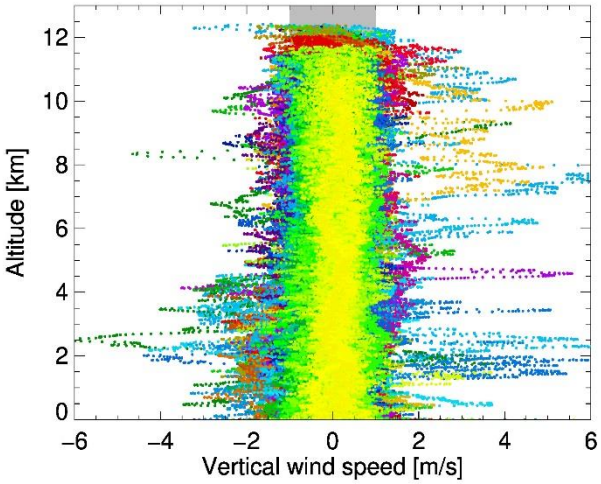

Figure 14: Vertical wind speed profiles. The grey shaded area indicates the estimated uncertainty for vertical winds derived by this method.

References

Vömel, H., I. Suhr, and G. Granger, 2019, NCAR/EOL/ISF Dropsonde NetCDF Data Files, UCAR/NCAR - Earth Observing Laboratory. https://doi.org/10.26023/54wh-rj45

Vömel, H., Goodstein, M., Tudor, L., Witte, J., Fuchs-Stone, Ž., Sentić, S., Raymond, D., Martinez-Claros, J., Juračić, A., Maithel, V., and Whitaker, J. W.: High-resolution in situ observations of atmospheric thermodynamics using dropsondes during the Organization of Tropical East Pacific Convection (OTREC) field campaign , Earth Syst. Sci. Data, 13, 1107–1117, https://doi.org/10.5194/essd-13-1107-2021, 2021

Wang, J., Bian, J., Brown, W. O., Cole, H., Grubišić, V., and Young, K.: Vertical Air Motion from T-REX Radiosonde and Dropsonde Data, J. Atmos. Ocean. Tech., 26, 928–942, https://doi.org/10.1175/2008JTECHA1240.1, 2009.

Appendix A: Listing of all sounding

#	Research Flight	Sounding	Latitude [°]	Longitude [°]	Altitude [km]	Fall rate [m/s]	Comment
1	TF01	20220616_165700	33.60426	-123.81334	11.4	-12.7	
2	TF01	20220616_170342	33.90003	-124.57398	11.4	-12.8	
3	TF01	20220616_170637	34.12491	-124.81310	11.4	-13.0	
4	TRANSIT	20220903_153935	31.78225	-52.32290	12.5	-13.1	
5	TRANSIT	20220903_162306	29.39512	-45.93676	12.5	-13.3	
6	TRANSIT	20220903_165841	27.32918	-40.78108	12.5	-13.7	
7	TRANSIT	20220903_172034	25.88087	-37.75126	12.5	-13.0	
8	TRANSIT	20220903_180702	22.45108	-32.06343	12.6	-13.3	
9	RF01	20220906_112953	16.22268	-25.76045			Failed at launch
10	RF01	20220906_113333	16.26886	-26.22385	7.1	-11.7	
11	RF01	20220906_120130	17.02641	-29.51992	7.1	-12.1	
12	RF01	20220906_120858	17.57538	-30.23541	7.1	-12.1	
13	RF01	20220906_122907	18.93803	-32.18033	7.1	-11.6	
14	RF01	20220906_123630	18.90181	-32.97014	4.3	-11.3	
15	RF01	20220906_131540	16.42868	-33.05718	9.6	-12.3	
16	RF01	20220906_133330	14.45955	-34.08526	11.9	-13.0	
17	RF01	20220906_134012	13.68347	-34.46119	12.0	-12.6	
18	RF01	20220906_134547	13.03356	-34.77345	12.0	-12.8	
19	RF01	20220906_135546	11.87347	-35.32688	11.9	-13.0	
20	RF01	20220906_140631	10.66223	-35.02459	11.9	-13.2	
21	RF01	20220906_141520	9.65286	-34.52265	12.0	-13.4	
22	RF01	20220906_142556	8.42806	-33.91771	11.9	-13.0	
23	RF01	20220906_144342	6.39971	-32.89032	11.9	-13.6	
24	RF01	20220906_144944	5.70791	-32.54511	11.9	-13.1	
25	RF01	20220906_145315	5.29387	-32.33946	11.9	-12.7	
26	RF01	20220906_145941	5.03414	-31.80971	11.9	-13.0	
27	RF01	20220906_150942	5.48904	-30.65941	11.9	-12.9	
28	RF01	20220906_151833	6.09982	-29.91715	11.9	-13.1	
29	RF01	20220906_152140	6.47318	-29.92264	11.9	-13.4	
30	RF01	20220906_152448	6.84465	-29.92693	11.9	-13.7	
31	RF01	20220906_153647	8.29742	-29.94410	11.9	-12.8	
32	RF01	20220906_155532	10.63150	-29.72214	11.9	-13.2	

#	Research Flight	Sounding	Latitude [°]	Longitude [°]	Altitude [km]	Fall rate [m/s]	Comment
33	RF01	20220906_160920	12.38314	-29.45194	12.6	-13.3	
34	RF01	20220906_161626	13.25346	-29.52799	12.6	-13.2	
35	RF01	20220906_162154	13.90852	-29.82462	12.6	-13.5	
36	RF01	20220906_162345	14.13752	-29.91440	12.6	-13.4	
37	RF01	20220906_162655	14.52530	-30.06443	12.6	-13.3	
38	RF01	20220906_164141	15.46652	-29.09918	12.6	-13.1	Partial fast fall
39	RF01	20220906_165717	14.87377	-28.73062	12.6	-12.6	
40	RF01	20220906_170142	14.91171	-29.33041	12.6	-13.4	
41	RF01	20220906_170457	14.94347	-29.77982	12.6	-13.9	
42	RF01	20220906_171732	15.37073	-29.52559	12.6	-14.0	Humidity sensor failed
43	RF02	20220907_122852	14.33304	-25.98455	11.0	-12.7	
44	RF02	20220907_124421	12.99030	-27.66186	11.0	-12.5	
45	RF02	20220907_130303	11.59504	-29.69622	11.0	-12.6	
46	RF02	20220907_131522	12.60578	-31.02728	11.0	-12.7	
47	RF02	20220907_132729	13.62064	-32.35491	9.7	-12.1	
48	RF02	20220907_133354	14.13528	-33.03400	9.7	-13.0	
49	RF02	20220907_133544	14.28446	-33.23210	9.7	-13.1	
50	RF02	20220907_133732	14.43243	-33.42899	9.7	-19.7	Fast fall
51	RF02	20220907_134225	14.87806	-33.93986	9.7	-12.2	
52	RF02	20220907_135426	16.09926	-35.08810	9.7	-12.2	
53	RF02	20220907_141802	18.43815	-37.34339	9.7	-12.5	
54	RF02	20220907_143006	19.63257	-38.52888	9.7	-12.9	
55	RF02	20220907_151045	15.31546	-39.81239	9.7	-12.3	
56	RF02	20220907_154321	11.37497	-40.18198	9.7	-12.3	
57	RF02	20220907_160231	13.12094	-38.29491	9.7	-12.9	
58	RF02	20220907_161604	14.41080	-37.00161	9.7	-12.5	
59	RF02	20220907_164216	15.73586	-34.76400	12.2	-12.3	
60	RF02	20220907_165103	16.62026	-35.32654	12.2	-13.3	
61	RF02	20220907_165747	17.05164	-34.56213	12.2	-12.9	
62	RF02	20220907_165853	17.12508	-34.43235			No launch-detect
63	RF02	20220907_170646	17.72987	-33.54658	11.9	-13.0	
64	RF02	20220907_171047	18.11028	-33.15777	11.9	-11.5	
65	RF02	20220907_171657	18.69547	-32.55575	11.9	-13.1	
66	RF02	20220907_172742	19.72733	-31.47841	11.9	-12.8	
67	RF02	20220907_173826	20.52675	-30.35042	11.9	-13.2	
68	RF02	20220907_175409	19.38520	-28.58540	11.9	-13.1	
69	RF02	20220907_180836	18.30477	-26.96560	11.9	-13.1	
70	RF02	20220907_182045	17.39153	-25.64089	8.5	-12.1	
71	RF03	20220909_131355	18.08195	-21.98296	10.0	-12.8	
72	RF03	20220909_132127	18.87846	-21.53767	10.0	-12.4	
73	RF03	20220909_132450	19.23883	-21.33600			Failed at launch
74	RF03	20220909_133042	19.88010	-20.97427	10.0	-12.6	
75	RF03	20220909_134324	21.00311	-19.91427	10.0	-12.6	
76	RF03	20220909_135853	21.81919	-18.78473	6.5	-11.9	
77	RF03	20220909_145322	24.15734	-19.31032			No launch-detect
78	RF03	20220909_150359	24.86031	-19.69486			No launch-detect
79	RF03	20220909_152950	21.47965	-19.65643	10.0	-12.6	
80	RF03	20220909_153120	21.27859	-19.66505			Failed at launch
81	RF03	20220909_160602	16.71278	-19.69832	10.0	-12.7	
82	RF03	20220909_161244	15.83954	-19.78123	10.0	-13.2	
83	RF03	20220909_162708	14.63722	-20.84501	12.2	-13.2	
84	RF03	20220909_162948	14.58075	-21.19520	12.2	-13.0	
85	RF03	20220909_163438	14.53302	-21.83910	12.3	-14.6	
86	RF03	20220909_163651	14.40441	-22.07226			No launch-detect
87	RF03	20220909_164943	15.34979	-21.59517	12.3	-12.8	
88	RF03	20220909_165847	14.77558	-20.92466	12.3	-13.1	

#	Research Flight	Sounding	Latitude [°]	Longitude [°]	Altitude [km]	Fall rate [m/s]	Comment
89	RF03	20220909_170002	14.62321	-20.87621			Failed at launch
90	RF03	20220909_171618	13.61034	-22.46412	12.2	-13.2	
91	RF03	20220909_175820	12.03672	-27.60057	12.2	-13.9	
92	RF03	20220909_181320	10.42088	-27.20730	12.2	-12.9	
93	RF03	20220909_183130	12.51000	-26.91891	12.5	-13.0	
94	RF03	20220909_183329	12.75032	-26.87994	12.5	-13.1	
95	RF03	20220909_183728	13.25003	-26.91599	12.5	-13.7	
96	RF03	20220909_183817	13.35268	-26.92509	12.5	-13.1	
97	RF03	20220909_184747	12.90825	-26.63498	12.5	-13.8	
98	RF03	20220909_184951	12.65711	-26.57473	12.5	-13.0	
99	RF03	20220909_192102	12.95357	-24.18108	10.0	-12.8	
100	RF03	20220909_193321	14.34300	-24.42398	10.0	-12.9	
101	RF03	20220909_193811	14.97372	-24.53607			No launch-detect
102	RF03	20220909_194900	16.32534	-24.77760	10.0	-12.3	
103	RF04	20220910_144824	12.46571	-27.54873	11.9	-13.2	
104	RF04	20220910_145619	11.68808	-28.31228	11.9	-13.0	
105	RF04	20220910_151213	10.45487	-30.11593	11.9	-13.2	
106	RF04	20220910_153514	8.37862	-32.44211	11.9	-13.2	
107	RF04	20220910_154826	7.16274	-33.58057	11.9	-12.6	
108	RF04	20220910_155212	6.65789	-33.56426	11.9	-13.5	
109	RF04	20220910_155729	5.93948	-33.54281	11.9	-12.9	
110	RF04	20220910_160028	5.53145	-33.53062	11.9	-12.4	
111	RF04	20220910_160326	5.12426	-33.51843	11.9	-12.3	
112	RF04	20220910_165853	3.91946	-31.72408			No launch-detect
113	RF04	20220910_170708	4.93853	-31.59016	11.9	-12.5	
114	RF04	20220910_170856	5.17130	-31.62586	11.9	-13.9	
115	RF04	20220910_172753	6.71574	-32.09536	11.9	-12.7	
116	RF04	20220910_172900	6.62458	-32.20402	11.9	-13.0	
117	RF04	20220910_173117	6.44348	-32.43284	11.9	-12.8	
118	RF04	20220910_185722	5.05817	-29.37470	11.9	-13.2	
119	RF04	20220910_191148	4.52431	-27.62941	11.9	-13.3	
120	RF04	20220910_193216	5.07053	-26.11090	11.9	-13.3	
121	RF04	20220910_194451	6.77729	-26.39554			No launch-detect
122	RF04	20220910_194847	7.27964	-26.47963	9.7	-12.5	
123	RF04	20220910_195037	7.51273	-26.51864			No launch-detect
124	RF04	20220910_202129	11.51659	-27.19116	9.7	-11.8	
125	RF04	20220910_202853	12.47068	-27.36059	9.7	-12.9	
126	RF04	20220910_203600	13.38598	-27.52436	9.7	-12.4	
127	RF05	20220914_100038	14.06765	-21.78314	8.1	-12.3	
128	RF05	20220914_100240	13.83731	-21.67737			No launch-detect
129	RF05	20220914_101158	12.74380	-21.26627	8.1	-12.4	
130	RF05	20220914_101326	12.56655	-21.21458			No launch-detect
131	RF05	20220914_102703	10.92860	-20.73757			No launch-detect
132	RF05	20220914_104056	9.24517	-20.21759	8.1	-11.8	
133	RF05	20220914_104554	8.69656	-19.97345			No launch-detect
134	RF05	20220914_105739	7.73146	-19.27826	8.1	-11.5	
135	RF05	20220914_110657	8.18190	-18.28680			No launch-detect
136	RF05	20220914_113501	10.44422	-17.15120	11.6	-12.8	
137	RF05	20220914_114500	11.54869	-17.81553	11.6	-13.5	
138	RF05	20220914_115120	12.23911	-18.30099	11.6	-12.6	
139	RF05	20220914_120116	13.52091	-18.60809	11.6	-13.0	
140	RF05	20220914_121728	15.59818	-19.05424	11.6	-12.9	
141	RF05	20220914_122949	15.75079	-18.01518	11.6	-13.2	
142	RF05	20220914_125042	13.65120	-17.71305	7.8	-11.8	
143	RF05	20220914_130420	12.09595	-17.22725	7.8	-11.1	
144	RF05	20220914_132000	10.55872	-16.24655	6.6	-12.0	

#	Research Flight	Sounding	Latitude [°]	Longitude [°]	Altitude [km]	Fall rate [m/s]	Comment
145	RF05	20220914_133432	9.29272	-15.85688	6.4	-12.1	
146	RF05	20220914_134326	8.86391	-16.73956	6.4	-12.2	
147	RF05	20220914_135257	8.61397	-17.64525	6.4	-11.2	
148	RF05	20220914_142106	11.42201	-19.49627	11.9	-13.0	
149	RF05	20220914_142805	12.18298	-20.01331	11.9	-12.8	
150	RF05	20220914_145026	14.09855	-21.37751	12.5	-13.4	
151	RF05	20220914_145550	14.09889	-20.70923	12.6	-12.9	
152	RF05	20220914_151934	13.53190	-18.07783	12.5	-12.7	
153	RF05	20220914_153201	12.28838	-17.96145	12.5	-13.4	
154	RF05	20220914_154350	12.30297	-19.54657	12.5	-13.3	
155	RF05	20220914_155230	12.93503	-20.37792	12.5	-13.1	
156	RF05	20220914_160428	14.20635	-21.31674	11.6	-13.7	
157	RF06	20220915_155735	18.34871	-21.22267	9.7	-12.9	
158	RF06	20220915_160733	19.22595	-20.17985			No launch-detect
159	RF06	20220915_161437	19.93092	-19.52150	9.7	-12.4	
160	RF06	20220915_163005	20.83815	-18.43609	9.7	-12.3	
161	RF06	20220915_164009	19.63978	-18.00007	9.7	-12.8	
162	RF06	20220915_174149	17.91836	-17.99990	9.7	-12.5	
163	RF06	20220915_175125	16.67055	-17.99973	9.7	-12.4	
164	RF06	20220915_175639	15.98261	-18.00013			No launch-detect
165	RF06	20220915_180025	15.48197	-17.99973	9.7	-12.9	
166	RF06	20220915_181452	14.00259	-18.53840	9.7	-12.5	
167	RF06	20220915_182512	14.00465	-20.00387	11.9	-13.6	
168	RF06	20220915_183514	14.24206	-21.19057	11.9	-13.4	
169	RF06	20220915_184826	15.95112	-21.50076	11.9	-13.1	
170	RF06	20220915_193002	18.99279	-22.05248	12.0	-13.2	
171	RF06	20220915_195249	21.07040	-22.85774	12.0	-12.4	
172	RF07	20220916_134044	14.75275	-26.43002	11.3	-13.2	
173	RF07	20220916_135340	13.85084	-27.86905	11.3	-13.1	
174	RF07	20220916_140352	13.14943	-29.01850	11.3	-13.6	
175	RF07	20220916_141117	12.56802	-29.76866	11.3	-13.7	
176	RF07	20220916_142226	11.30390	-30.47419	11.3	-13.1	
177	RF07	20220916_143342	9.99241	-31.19843	11.3	-13.5	
178	RF07	20220916_144808	8.44917	-31.50244	11.9	-13.3	
179	RF07	20220916_150300	8.42857	-30.17481	12.3	-13.1	
180	RF07	20220916_151730	9.66385	-29.87423	12.2	-13.3	
181	RF07	20220916_152223	9.13908	-29.56575	12.2	-13.9	
182	RF07	20220916_153809	8.61998	-28.04209	12.2	-13.7	
183	RF07	20220916_155505	9.06509	-26.03846	12.2	-13.7	
184	RF07	20220916_161920	9.25358	-24.98051	12.3	-13.4	
185	RF07	20220916_162659	8.54462	-25.23233	12.2	-13.6	
186	RF07	20220916_164015	9.31297	-26.83359	12.2	-13.6	
187	RF07	20220916_171129	9.91070	-28.38129	12.2	-14.0	
188	RF07	20220916_172129	10.96470	-29.07120	12.2	-14.1	
189	RF07	20220916_173550	10.20458	-29.48250	12.2	-13.1	
190	RF07	20220916_174606	10.11137	-29.47237	12.2	-13.1	
191	RF07	20220916_180341	9.68325	-28.26267	12.3	-13.3	Partial fast fall
192	RF07	20220916_181526	9.54947	-29.29112			No launch-detect
193	RF07	20220916_182256	9.93542	-28.47467	12.2	-14.4	
194	RF07	20220916_183130	10.49177	-27.56367	12.2	-13.1	
195	RF07	20220916_183732	10.89535	-26.92989	12.3	-13.4	
196	RF07	20220916_184855	11.75692	-25.82251	12.3	-12.7	
197	RF07	20220916_185720	12.40768	-24.97656	11.3	-13.2	
198	RF07	20220916_192135	15.13268	-24.57440			No launch-detect
199	RF07	20220916_192240	15.27020	-24.59864			Failed at launch
200	RF07	20220916_193009	16.20518	-24.76490	10.7	-13.1	

#	Research Flight	Sounding	Latitude [°]	Longitude [°]	Altitude [km]	Fall rate [m/s]	Comment
201	RF08	20220920_052956	14.18901	-21.75842	8.0	-12.1	
202	RF08	20220920_054632	12.36340	-20.91488	8.0	-11.8	
203	RF08	20220920_055924	10.94702	-20.27527	8.0	-12.5	
204	RF08	20220920_061536	9.15419	-19.47619	8.0	-12.2	
205	RF08	20220920_062608	7.99616	-18.96429	8.0	-12.6	
206	RF08	20220920_062929	7.61930	-18.79877			No launch-detect
207	RF08	20220920_063502	7.30042	-18.39970	8.0	-12.3	
208	RF08	20220920_064953	8.30017	-16.88496	11.9	-12.9	
209	RF08	20220920_065544	8.68280	-16.30148	11.9	-10.3	Late launch detect
210	RF08	20220920_065850	8.88811	-15.98768	11.9	-13.1	
211	RF08	20220920_071139	9.78333	-15.11341	11.9	-13.0	
212	RF08	20220920_071842	10.30106	-15.91404	11.9	-13.5	
213	RF08	20220920_072700	10.71528	-16.83792	12.2	-13.9	
214	RF08	20220920_073340	10.29093	-17.61847	12.2	-13.8	
215	RF08	20220920_074054	9.82023	-18.47729	12.2	-13.7	
216	RF08	20220920_074441	9.57282	-18.92487			No launch-detect
217	RF08	20220920_074748	9.36876	-19.29371	12.2	-13.8	
218	RF08	20220920_075910	9.40704	-20.40333	12.2	-13.6	
219	RF08	20220920_080808	10.37212	-20.59765	12.2	-13.0	
220	RF08	20220920_081452	10.70738	-19.85092	12.2	-13.0	
221	RF08	20220920_082129	11.03096	-19.12102	12.2	-13.3	
222	RF08	20220920_082522	11.21543	-18.70249			No launch-detect
223	RF08	20220920_083002	11.43728	-18.19628	12.2	-13.4	
224	RF08	20220920_084657	12.43755	-17.33351	12.2	-13.0	
225	RF08	20220920_085438	13.06738	-18.13208	12.2	-13.1	
226	RF08	20220920_090735	14.05340	-19.39756	7.8	-12.3	
227	RF09	20220922_052442	14.61096	-21.21494	8.0	-12.3	
228	RF09	20220922_054052	12.89675	-20.28626	8.0	-11.8	
229	RF09	20220922_060236	10.42671	-19.49421	8.0	-11.8	
230	RF09	20220922_061308	9.50592	-18.66732	8.0	-11.8	
231	RF09	20220922_062220	8.75027	-18.06238	8.0	-12.9	
232	RF09	20220922_063014	9.13891	-17.17695	8.0	-11.5	
233	RF09	20220922_063908	9.57699	-16.17308	8.0	-12.1	
234	RF09	20220922_065024	10.30672	-15.57312	11.4	-12.8	
235	RF09	20220922_065402	10.58069	-15.95610	11.9	-16.6	Early data loss
236	RF09	20220922_070250	11.31832	-16.83432	11.9	-12.9	
237	RF09	20220922_070631	11.41651	-17.28802	11.9	-13.8	
238	RF09	20220922_071332	11.14700	-18.18203	11.9	-12.5	
239	RF09	20220922_072340	10.72918	-19.54468	11.9	-12.7	
240	RF09	20220922_073503	11.16091	-20.68829	11.9	-13.3	
241	RF09	20220922_074024	11.75880	-21.05616	11.9	-13.1	
242	RF09	20220922_074725	12.29731	-20.93084	11.9	-12.5	
243	RF09	20220922_075255	12.35207	-20.25656	11.9	-13.9	
244	RF09	20220922_080030	12.42708	-19.31809	11.9	-12.4	Partial fast fall
245	RF09	20220922_081200	12.53506	-17.85759	11.9	-14.0	
246	RF09	20220922_082024	13.00301	-17.72524	11.9	-12.9	
247	RF09	20220922_083439	14.14764	-19.14557	8.1	-12.2	
248	RF09	20220922_085740	15.63131	-20.37586	8.1	-11.9	
249	RF09	20220922_092126	15.94803	-17.71872	8.1	-12.5	
250	RF09	20220922_092759	16.72445	-17.72610	8.1	-11.2	
251	RF09	20220922_093606	17.50208	-17.98616	8.1	-10.7	
252	RF09	20220922_100103	17.83012	-20.99968	8.1	-12.2	
253	RF09	20220922_102303	18.17156	-18.49188			Failed at launch
254	RF09	20220922_103846	18.16864	-18.03921	8.1	-12.3	
255	RF09	20220922_105355	18.17242	-20.01022	8.1	-12.2	
256	RF10	20220923_083217	18.88636	-25.19028	10.9	-12.5	

#	Research Flight	Sounding	Latitude [°]	Longitude [°]	Altitude [km]	Fall rate [m/s]	Comment
257	RF10	20220923_085146	16.44293	-24.98566	10.3	-12.6	
258	RF10	20220923_091243	14.02233	-24.74035	11.6	-12.9	
259	RF10	20220923_092645	14.16704	-22.94134	11.6	-13.0	
260	RF10	20220923_093325	14.16790	-22.10638	11.6	-13.5	
261	RF10	20220923_094059	14.03502	-21.25700			No launch-detect
262	RF10	20220923_094640	13.36332	-21.52153	11.6	-13.3	
263	RF10	20220923_095146	13.42804	-22.01111	11.6	-13.3	
264	RF10	20220923_095834	14.02353	-22.60214			PTU sensor failed
265	RF10	20220923_100754	14.14379	-22.59521			No launch-detect
266	RF10	20220923_101157	14.15417	-22.07668	11.6	-13.1	
267	RF10	20220923_103002	15.13847	-20.16695	11.6	-13.2	
268	RF10	20220923_103728	16.08879	-20.16661	11.6	-13.1	
269	RF10	20220923_104454	17.03121	-20.16661	11.6	-13.0	
270	RF10	20220923_105242	18.01466	-20.16678	11.6	-12.7	
271	RF10	20220923_110018	19.01304	-20.16661	11.6	-12.8	
272	RF10	20220923_111043	19.72046	-20.70803	11.6	-13.0	
273	RF10	20220923_111500	19.54039	-21.22919	11.6	-13.6	
274	RF10	20220923_112201	19.26745	-22.10260	11.6	-13.1	
275	RF10	20220923_113517	18.93717	-22.41022	11.6	-13.5	
276	RF10	20220923_114018	18.68139	-21.78572	11.6	-13.6	
277	RF10	20220923_114510	18.44244	-21.20585	11.6	-12.8	
278	RF10	20220923_115425	17.88317	-20.52452	11.6	-13.4	
279	RF10	20220923_115927	17.51238	-21.09066	11.6	-13.8	
280	RF10	20220923_120516	17.08803	-21.73388	11.6	-13.0	
281	RF10	20220923_121351	16.57030	-21.89180	11.6	-13.0	
282	RF10	20220923_121756	16.46765	-21.38197	11.6	-13.0	
283	RF10	20220923_122255	16.33616	-20.74545	11.6	-13.4	
284	RF10	20220923_124223	14.86914	-21.32378	11.6	-14.0	
285	RF10	20220923_124620	15.21589	-21.69611	11.6	-14.3	
286	RF10	20220923_125022	15.56711	-22.09076	11.6	-13.6	
287	RF10	20220923_125155	15.68951	-22.26414	11.6	-12.7	
288	RF10	20220923_125752	15.70822	-22.87325			No launch-detect
289	RF10	20220923_125838	15.63234	-22.92812	11.6	-13.5	
290	RF10	20220923_130413	15.11375	-22.75921	11.6	-13.2	
291	RF10	20220923_130841	14.75584	-22.31632	11.6	-13.2	
292	RF10	20220923_131210	14.46608	-21.97231	11.6	-13.1	
293	RF10	20220923_132359	15.31529	-22.15221	11.3	-13.3	
294	RF10	20220923_133830	15.02728	-22.55929			No launch-detect
295	RF10	20220923_134112	14.80408	-22.28611	10.3	-12.4	
296	RF10	20220923_134440	14.51757	-21.93695	10.3	-11.8	
297	RF10	20220923_135114	14.84528	-21.27691	10.3	-13.1	
298	RF10	20220923_135736	15.42257	-20.96483	10.3	-13.1	
299	RF11	20220926_053609	13.64571	-24.22932	9.3	-12.3	
300	RF11	20220926_055242	11.60757	-24.90910			PTU sensor failed
301	RF11	20220926_055332	11.50457	-24.94309	9.0	-12.9	
302	RF11	20220926_055732	11.01117	-25.10593			No launch-detect
303	RF11	20220926_060626	10.02863	-25.15303	9.0	-12.6	
304	RF11	20220926_061223	9.77755	-24.44064			No launch-detect
305	RF11	20220926_062906	9.05085	-22.41468	9.0	-12.2	
306	RF11	20220926_063916	8.60951	-21.22610	9.0	-11.7	
307	RF11	20220926_064936	8.14447	-19.99838	9.0	-12.6	
308	RF11	20220926_070400	8.49415	-18.73941	10.8	-12.2	
309	RF11	20220926_071144	9.41958	-18.45514	11.6	-12.3	
310	RF11	20220926_072222	10.59391	-18.37103	11.6	-13.0	
311	RF11	20220926_073246	10.99508	-19.69402	11.6	-13.3	
312	RF11	20220926_074044	11.29858	-20.71369	11.6	-12.4	

#	Research Flight	Sounding	Latitude [°]	Longitude [°]	Altitude [km]	Fall rate [m/s]	Comment
313	RF11	20220926_075134	12.44957	-20.98955	11.6	-13.3	
314	RF11	20220926_080106	13.05845	-20.05863			PTU sensor failed
315	RF11	20220926_080704	12.53214	-19.50777	11.6	-13.0	
316	RF11	20220926_081402	11.93098	-18.88275	11.6	-12.9	
317	RF11	20220926_082108	11.29500	-18.24016			No launch-detect
318	RF11	20220926_082324	11.07370	-18.39369	11.6	-12.5	
319	RF11	20220926_083007	10.43444	-18.98180	11.6	-13.7	
320	RF11	20220926_083900	9.80375	-19.84749	11.6	-13.3	
321	RF11	20220926_085546	10.97620	-21.50230	11.6	-12.9	
322	RF11	20220926_090432	11.10735	-20.99075	11.6	-13.8	
323	RF11	20220926_090832	10.76695	-20.78373	11.6	-13.9	
324	RF11	20220926_091234	10.61743	-20.29896	11.6	-12.9	
325	RF11	20220926_092210	10.33642	-19.12325	11.6	-13.7	
326	RF11	20220926_092607	10.11376	-18.73479			No launch-detect
327	RF11	20220926_094224	10.91440	-20.30788	11.6	-13.1	
328	RF11	20220926_094718	10.56782	-20.48487	11.6	-12.8	
329	RF11	20220926_102447	10.81862	-17.90016	11.6	-13.1	
330	RF11	20220926_102814	10.38277	-17.91647	11.6	-13.4	Humidity sensor failed
331	RF11	20220926_104156	10.45778	-17.23875	11.6	-12.7	
332	RF11	20220926_105453	11.70892	-17.96315			No launch-detect
333	RF11	20220926_110010	12.39121	-17.96969	11.0	-12.7	
334	RF11	20220926_111004	13.63609	-18.21688	9.7	-12.3	
335	RF11	20220926_111944	14.70640	-19.01802	9.7	-21.1	Fast fall
336	RF11	20220926_113340	16.07609	-20.29432	9.7	-13.0	
337	RF12	20220929_081449	16.15522	-22.43683	8.1	-11.9	
338	RF12	20220929_081727	16.45735	-22.51648	8.1	-11.9	
339	RF12	20220929_082225	17.02950	-22.66806	8.1	-12.3	
340	RF12	20220929_083446	16.97868	-23.49941	8.1	-11.9	
341	RF12	20220929_083915	16.44516	-23.39350	8.1	-12.1	
342	RF12	20220929_084201	16.11454	-23.32827	8.1	-12.1	
343	RF12	20220929_084917	15.57758	-23.84909	8.1	-12.5	
344	RF12	20220929_090405	14.83927	-24.99407	8.1	-12.0	
345	RF12	20220929_091403	13.62871	-24.97879	9.4	-12.5	
346	RF12	20220929_092456	12.16599	-25.20161	10.3	-12.6	
347	RF12	20220929_093121	11.28075	-25.33538			No launch-detect
348	RF12	20220929_093627	10.58567	-25.43936	10.3	-12.5	
349	RF12	20220929_094658	9.17788	-25.64964	10.3	-13.0	
350	RF12	20220929_101352	8.84966	-22.80144	10.5	-13.0	
351	RF12	20220929_102735	9.03505	-21.15091	11.6	-12.5	
352	RF12	20220929_104611	9.24980	-19.00034	11.6	-13.1	
353	RF12	20220929_111112	9.25409	-15.93824	11.6	-12.6	
354	RF12	20220929_113436	8.18070	-16.23264	11.6	-13.9	
355	RF12	20220929_120226	8.20936	-19.57815	11.6	-13.2	
356	RF12	20220929_121037	7.63224	-20.07803	11.6	-12.7	
357	RF12	20220929_123022	6.13741	-18.58475	11.6	-13.4	
358	RF12	20220929_124006	5.72582	-17.72623			No launch-detect
359	RF12	20220929_124353	5.95940	-17.33608	11.6	-12.6	
360	RF12	20220929_125546	6.79796	-16.42061	11.6	-12.7	
361	RF12	20220929_131241	8.57054	-17.53899	11.6	-13.6	
362	RF12	20220929_133813	9.99687	-20.11528	9.7	-13.0	
363	RF12	20220929_134923	10.45109	-21.14801			No launch-detect
364	RF12	20220929_135709	11.36158	-21.33150	9.7	-12.5	
365	RF12	20220929_141908	13.92191	-21.85490	9.7	-13.3	
366	RF12	20220929_144010	16.41684	-22.37726	9.7	-12.5	
367	RF12	20220929_145622	17.68370	-21.98433	9.7	-13.1	
368	RF12	20220929_150910	17.41482	-20.35965			No launch-detect

#	Research Flight	Sounding	Latitude [°]	Longitude [°]	Altitude [km]	Fall rate [m/s]	Comment
369	RF12	20220929_151624	17.25575	-19.43619	9.7	-12.8	
370	RF12	20220929_152946	16.65545	-18.13534	9.7	-12.4	
371	RF12	20220929_153204	16.36853	-18.24576			No launch-detect
372	RF12	20220929_153900	15.50858	-18.57874	9.7	-12.5	
373	RF13	20220930_090029	13.72261	-21.14508	10.6	-12.6	
374	RF13	20220930_091240	12.37043	-20.40453	10.6	-12.8	
375	RF13	20220930_092538	10.88436	-19.62982	11.6	-13.0	
376	RF13	20220930_093639	9.63141	-18.99210	11.6	-12.5	
377	RF13	20220930_094348	8.80537	-18.57616	11.6	-12.6	
378	RF13	20220930_095506	7.49817	-17.92643	11.6	-13.2	
379	RF13	20220930_100628	6.18496	-17.29712	11.6	-13.2	
380	RF13	20220930_101809	4.79828	-16.63656	11.6	-13.4	
381	RF13	20220930_102951	3.52215	-16.34903	9.0	-12.2	
382	RF13	20220930_103253	3.32678	-16.69362			No launch-detect
383	RF13	20220930_103824	2.96047	-17.33213	9.0	-12.5	
384	RF13	20220930_105250	2.41837	-18.87520	9.1	-12.9	
385	RF13	20220930_110023	3.38894	-19.10832	9.1	-12.3	
386	RF13	20220930_110721	4.28553	-19.32598	10.8	-13.7	
387	RF13	20220930_111058	4.71291	-19.43044			No launch-detect
388	RF13	20220930_111644	5.40407	-19.59995	11.9	-12.6	
389	RF13	20220930_112548	6.51026	-19.87427	11.9	-13.2	
390	RF13	20220930_112807	6.79602	-19.94538			No launch-detect
391	RF13	20220930_114329	8.44334	-20.62460	11.9	-12.4	
392	RF13	20220930_115702	7.99976	-22.15651	11.6	-12.2	
393	RF13	20220930_120731	6.65171	-22.00424	11.6	-13.0	
394	RF13	20220930_121103	6.20441	-21.95324			No launch-detect
395	RF13	20220930_121559	5.58226	-21.88236	11.6	-13.7	
396	RF13	20220930_122459	4.41977	-21.75156	11.9	-12.8	
397	RF13	20220930_123450	3.15771	-21.61165	9.0	-12.0	
398	RF13	20220930_124649	1.86665	-21.71688	9.0	-12.5	
399	RF13	20220930_130208	2.04929	-23.72583	9.0	-12.2	
400	RF13	20220930_131358	2.62796	-24.91562	9.0	-12.2	
401	RF13	20220930_132446	4.03490	-25.01209	11.9	-13.5	Humidity sensor failed
402	RF13	20220930_133316	5.14023	-25.08883	11.9	-12.8	
403	RF13	20220930_134822	7.04773	-25.21277	11.9	-13.0	
404	RF13	20220930_135302	7.61473	-25.14530	11.9	-13.2	
405	RF13	20220930_140056	8.58925	-25.03183	11.9	-13.1	
406	RF13	20220930_140548	9.20672	-24.95974	11.9	-12.6	
407	RF13	20220930_141046	9.84118	-24.88541	11.9	-13.1	
408	RF13	20220930_141737	10.62300	-24.69588			No launch-detect
409	RF13	20220930_142426	11.47522	-24.45608	11.9	-12.8	
410	Transit	20221002_085644	20.53602	-28.30662	10.9	-13.1	
411	Transit	20221002_090520	21.17683	-29.29848	10.9	-12.5	
412	Transit	20221002_095729	25.64261	-34.48488	10.9	-12.7	
413	Transit	20221002_102228	27.80073	-37.12641	10.9	-12.5	Humidity sensor failed
414	Transit	20221002_134406	37.09705	-65.78854	11.5	-12.8	